

Inhibition of Telomerase Activity by Preventing Proper Assemblage<sup>†</sup>

Brian R. Keppler and Michael B. Jarstfer\*

*School of Pharmacy, Division of Medicinal Chemistry and Natural Products, University of North Carolina, Chapel Hill, North Carolina 27599-7360**Received September 3, 2003; Revised Manuscript Received November 10, 2003*

**ABSTRACT:** Telomerase is a ribonucleoprotein complex that acts as a reverse transcriptase in the maintenance of chromosome ends. Because the vast majority of cancer cells require telomerase activity, telomerase has become a target for anticancer drug discovery. Here, we describe a new approach for targeting telomerase by blocking the association between the telomerase catalytic subunit, hTERT, and key elements of the human telomerase RNA subunit, hTR. By examining the effects of oligonucleotides that hybridize to various regions of hTR, we identified two regions of the RNA subunit that are sensitive to molecular interactions leading to telomerase inhibition. Oligonucleotides that hybridize to either the P3/P1 pairing region or to the CR4–CR5 domain of hTR, hTRas009, and hTRas010, respectively, inhibit telomerase activity when added to recombinant hTERT and hTR prior to assemblage. However, addition of hTRas009 or hTRas010 to preassembled telomerase resulted in little or no inhibition. We also examined the ability of hTRas009 and hTRas010 to inhibit binding of hTR and hTR fragments to hTERT. We found that hTRas009 inhibited ~50% of the maximum binding between the pseudoknot fragment of hTR (nucleotides 46–209) and hTERT, whereas hTRas010 inhibited over 90% of the maximum binding between the CR4–CR5 fragment of hTR (nucleotides 243–328) and hTERT. In addition, neither oligonucleotide was able to appreciably inhibit the binding of full-length hTR to hTERT, although both oligonucleotides used in conjunction decreased binding by ~50%. We propose that the P3/P1 pairing region and CR4–CR5 domain represent viable targets to inhibit telomerase by perturbing proper assemblage of the active complex.

Human chromosomes end in DNA–protein complexes called telomeres, which guard the chromosome ends from degradation and aberrant recombination (1). Human telomeric DNA is composed of the simple repeated sequence (TTAGGG)<sub>n</sub>, which is not replicated efficiently by the normal DNA replication machinery. Instead, telomeric DNA is maintained by a specialized RNA-dependent DNA polymerase called telomerase (2). The minimally active human telomerase complex is composed of two subunits: a protein (hTERT)<sup>1</sup> and an RNA (hTR) (3–5). The protein subunit employs its reverse transcriptase activity to extend telomeric DNA by using a small portion of the RNA subunit as a template for the G-rich sequence addition. The maintenance of telomeric DNA is vital for tumor growth, and the majority of cancer cell types require telomerase-mediated telomere extension for survival (6). When telomerase activity is inhibited in telomerase positive cancer cells, telomere maintenance is disrupted leading to senescence or cell death (2). Because of the general requirement for telomerase in cancers, it has the potential to be a universal anticancer drug target.

Several methods to affect telomerase inhibition have been documented (7, 8). These include reverse transcriptase inhibitors (9–12), G-quadruplex-stabilizing compounds (13), natural products (14–16), molecules screened from synthetic libraries (17–19), and antisense oligonucleotides directed at the RNA subunit, particularly the template (20). These inhibitors generally target either the telomerase-catalyzed primer extension reaction or the telomerase primer (for some G-quadruplex-interacting molecules). One aspect of telomerase biochemistry that has not been a major focus for drug discovery is assemblage of the ribonucleoprotein complex. We have therefore initiated a program to investigate the feasibility of inhibiting telomerase assemblage. In our initial efforts, we have specifically addressed the possibility of targeting hTR with oligonucleotides that block assemblage of the holoenzyme. Previous studies documented that non-templating portions of hTR can be targets for PNA-based inhibitors though inhibition of assemblage has not specifically been examined (21).

The telomerase RNA subunit has been identified from various organisms, including ciliates, mammals, and yeast (5, 22–28). Extensive, comparative phylogenetic analysis of the vertebrate telomerase RNA allowed a proposed secondary structure of hTR (22). Vertebrate telomerase RNAs contain several conserved regions including the template-containing pseudoknot and the CR4–CR5 domains (Figure 1). Previous studies have shown that the pseudoknot and CR4–CR5 domains are essential for telomerase activity and interact separately with hTERT (23, 29–34). In addition, Chen et al. revealed the presence of an additional secondary structure

<sup>†</sup> This work was supported by a grant from the North Carolina Pharmacy Foundation. M.B.J. was supported in part by a R. J. Reynolds Fund Award from the University of North Carolina. B.R.K. is a fellow of the American Foundation for Pharmaceutical Education.

\* To whom correspondence should be addressed. Tel: 919-966-6422. Fax: 919-966-0204. E-mail: jarstfer@unc.edu. School of Pharmacy, Division of Medicinal Chemistry and Natural Products, CB # 7360, University of North Carolina, Chapel Hill, NC 27599-7360.

<sup>1</sup> Abbreviations: hTERT, human telomere reverse transcriptase; hTR, human telomerase RNA.

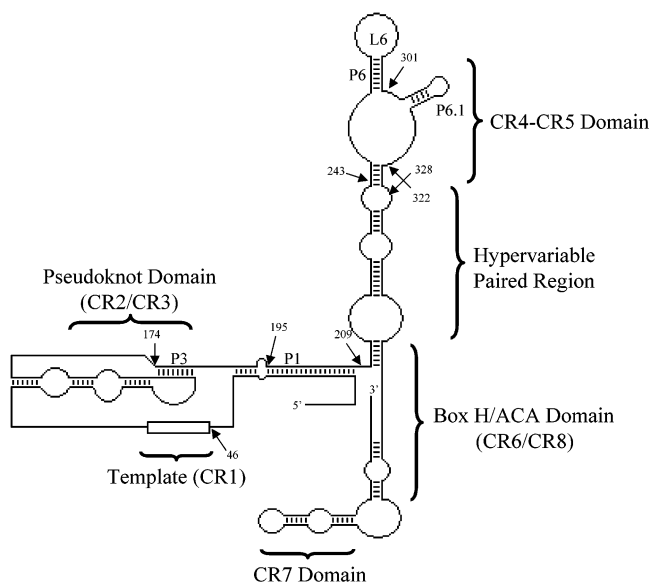


FIGURE 1: Human telomerase RNA. Conserved regions (CR) of hTR are indicated. Pairing regions (P) indicated include the P3 pairing region, which is part of the pseudoknot domain, and the P6.1 stem-loop, which is part of the CR4–CR5 domain. Arrows indicate nucleotides that are referred to in the text. The structure was adapted from Chen and Greider (22, 23).

within the CR4–CR5 domain of hTR, the P6.1 stem-loop (nucleotides 302–314), which appears to be essential for telomerase activity as well as for binding to hTERT (23). The roles of hTR were further extended by the work of Ly et al. (35). They showed that hTR can homodimerize via the P3 pairing region to form a trans-pseudoknot and that mutations preventing the P3-trans interaction led to loss of enzymatic activity but did not appear to prevent binding of hTR to hTERT (35). Here, we confirm that the CR4–CR5 domain and the P3/P1 pairing region both interact autonomously with hTERT and report that targeted disruption of these interactions prior to holoenzyme assembly disrupts telomerase activity.

## MATERIALS AND METHODS

**Oligonucleotides.** All oligonucleotides were purchased from and purified by Integrated DNA Technologies (Coralville, Iowa). Oligonucleotide concentrations were determined by UV absorbance at 260 nm using the molar extinction coefficient provided by Integrated DNA Technologies.

**pET-28c-hTERT and phTR+HH Expression Plasmids.** An hTERT plasmid (pCl-neo-hTERT) was a gift from Dr. Lorel Colgin (Children's Medical Research Institute, Westmead Australia) and CAMBIA (Canberra Australia) (36). The hTERT-containing insert from this plasmid was subcloned into the *EcoRI* and *SalI* sites of the T7-tag-containing plasmid pET-28c (Novagen) to give the construct pET-28c-hTERT. phTR+HH, a plasmid designed for in vitro transcription of human telomerase RNA with a self-cleaving hammerhead ribozyme that generates the natural 5' end, was a gift from Dr. Jamie Sperger (University of Colorado, Boulder).

**In Vitro Transcription and Purification of hTR.** A total of 15  $\mu$ g of phTR+HH was linearized by digestion with *FokI* followed by extraction with phenol/chloroform/isoamyl alcohol, precipitation with ethanol, and resuspension in a

suitable volume of TE (10 mM Tris-HCl, pH 7.5, and 1 mM EDTA). In vitro transcription was carried out at 37 °C for 18 h using the linearized DNA, 0.32 units/ $\mu$ L T7 RNA polymerase (Promega), 1 $\times$  transcription-optimized buffer (Promega), 10 mM DTT, 0.8 units/ $\mu$ L RNasin (Fisher Scientific), 5 mM MgCl<sub>2</sub>, and 1 mM each NTP. After transcription, the magnesium–inorganic diphosphate complexes were removed by centrifugation for 2 min at 22000g. Cleavage by the hammerhead ribozyme was initiated by the addition of MgCl<sub>2</sub> to a final concentration of 12 mM followed by incubation at 45 °C for 1 h. The entire reaction was then treated with 15 units of RQ1-DNase (Promega) for 20 min at 37 °C followed by extraction with phenol/chloroform/isoamyl alcohol and ethanol precipitation. The RNA was resuspended in a suitable volume of denaturing loading buffer (7 M urea/10% glycerol/1 $\times$  TBE) and purified on a 4% denaturing polyacrylamide gel. The RNA was recovered using a modified version of the “crush and soak” method (37). Briefly, the RNA was located in the gel by UV shadowing, cut out, crushed by passing through a sterile plastic syringe, and extracted into 2 vol of 1 $\times$  TEN (10 mM Tris-HCl, pH 7.5, 1 mM EDTA, and 200 mM NaCl) at 4 °C for 16 h. After centrifugation, the supernatant was collected and a second extraction was performed with 2 vol of 1 $\times$  TEN at room temperature for 1 h. The combined supernatants were filtered through a Whatman GF/C filter, precipitated with ethanol, and resuspended in a suitable volume of TE.

**Synthesis of hTERT.** hTERT was transcribed and translated using the TNT Coupled Reticulocyte Lysate Systems kit (Promega). A 400  $\mu$ L reaction contained 8  $\mu$ g of pET-28c-hTERT, 16  $\mu$ L of [<sup>35</sup>S]-methionine (1175 Ci/mmol, 10  $\mu$ Ci/ $\mu$ L; Perkin-Elmer), and other components provided in the kit as described by the manufacturer. The reaction was incubated at 30 °C for 90 min, flash-frozen in a dry ice/ethanol bath, and stored at –80 °C. hTERT used in the direct telomerase assay and the assemblage assay was made without [<sup>35</sup>S]-methionine as described by the manufacturer. A reticulocyte lysate reaction with pET-28c (empty vector control) in place of pET-28c-hTERT served as a negative control in several experiments.

**Reconstitution of Telomerase.** Preassembled telomerase was prepared by adding 4  $\mu$ g of in vitro transcribed hTR to the 400  $\mu$ L reticulocyte lysate reaction prior to incubation for 90 min at 30 °C. Direct telomerase assays contained 10  $\mu$ L of preassembled telomerase. Reconstitution of telomerase in the assemblage assay was initiated by combining 10  $\mu$ L (~50 fmol) of hTERT from a reticulocyte lysate reaction, 212.5 ng of in vitro transcribed hTR, and the appropriate amount of water or oligonucleotide inhibitor to a final volume of 15  $\mu$ L followed by incubation at 30 °C for 90 min. The preassembled telomerase complex and the hTERT protein were used in assays without further purification from the reticulocyte lysate.

**Direct Telomerase Assay.** Telomerase activity was measured using a modification of a previously described direct assay (34). Each 25  $\mu$ L reaction contained 50 mM Tris-HCl, pH 8.0, 50 mM KCl, 1 mM MgCl<sub>2</sub>, 5 mM  $\beta$ -mercaptoethanol, 1 mM spermidine, 1  $\mu$ M human telomere primer (5'-TTAGGGTTAGGGTTAGGG), 0.5 mM dATP, 0.5 mM dTTP, 2.9  $\mu$ M dGTP, 0.33  $\mu$ M [ $\alpha$ -<sup>32</sup>P]-dGTP (3000 Ci/mmol, 10  $\mu$ Ci/ $\mu$ L; Perkin-Elmer), and 10  $\mu$ L of preassembled

telomerase. Inhibition studies also included varying amounts of oligonucleotide inhibitor. Primer extension was carried out at 30 °C for 90 min. After the addition of a  $^{32}\text{P}$ -labeled loading control (114 nucleotide, 5'-end labeled DNA oligonucleotide, 1000 cpm per reaction), the primer extension products were extracted with phenol/chloroform/isoamyl alcohol and ethanol precipitated in the presence of 0.6 M  $\text{NH}_4\text{OAc}$  and 35 ng/ $\mu\text{L}$  glycogen. Products were precipitated at -80 °C in 2.5 vol of absolute ethanol for 30 min followed by centrifugation at 22 000g at 4 °C for 25 min and washing with 2 vol of 70% ethanol. Pellets were resuspended in a suitable volume of TE, and ethanol precipitation was repeated to ensure the removal of all unincorporated [ $\alpha$ - $^{32}\text{P}$ ]-dGTP. The final pellets were dissolved in a formamide loading buffer containing 40% formamide, 10 mM Tris-HCl, pH 8.0, 10 mM EDTA, 0.05% xylene cyanol, and 0.05% bromophenol blue. The products were heated at 95 °C for 5 min and resolved on a prewarmed, 0.4 mm thick, 20 × 20 cm, 10% polyacrylamide/7 M urea/1 × TBE gel. A small amount of the human telomere primer was labeled with [ $\gamma$ - $^{32}\text{P}$ ]-ATP and T4 polynucleotide kinase (Fisher) and loaded in a separate lane to be used as a marker for the start of primer elongation. The gel was run at 800 V for 1 h in 1 × TBE. After drying the gel and exposing it to a phosphorimager screen (Molecular Dynamics) overnight, telomerase activity was imaged using a phosphorimager (Molecular Dynamics Storm 860) and quantified with ImageQuant (version 5.2). The intensities of each band in each sample were summed and normalized to the loading control.

**Assemblage Assay.** Each 25  $\mu\text{L}$  reaction contained 50 mM Tris-HCl, pH 8.0, 50 mM KCl, 1 mM  $\text{MgCl}_2$ , 5 mM  $\beta$ -mercaptoethanol, 1 mM spermidine, 1  $\mu\text{M}$  human telomere primer (5'-TTAGGGTTAGGGTTAGGG), 0.5 mM dATP, 0.5 mM dTTP, 2.9  $\mu\text{M}$  dGTP, 0.33  $\mu\text{M}$  [ $\alpha$ - $^{32}\text{P}$ ]-dGTP (3000 Ci/mmol, 10  $\mu\text{Ci}/\mu\text{L}$ ; Perkin-Elmer), and 15  $\mu\text{L}$  of reconstituted telomerase. Inhibition studies also included varying amounts of oligonucleotide inhibitor. Primer extension was carried out at 30 °C for 90 min, and the samples were processed as described for the direct telomerase assay.

**Synthesis of  $^{32}\text{P}$ -Labeled CR4–CR5 and Pseudoknot RNA Fragments and Full-Length hTR.** RNA fragments were generated using a modification of the protocol described by Chen et al. (34). The desired DNA templates were amplified by PCR using the phTR+HH plasmid described above. The pseudoknot PCR fragment (nucleotides 46–209) was synthesized using the T7 promoter-containing forward primer 5'-GGGTACCTAATACGACTCACTATAGGCTAACCC-TAACTGAGAAGGGCGTAGGCGCCGTG-3' and the reverse primer 5'-CCCCGGGAGGGGCGAACGGGCCA-3'. The CR4–CR5 PCR fragment (nucleotides 243–328) was synthesized using the T7 promoter-containing forward primer 5'-GCGGGAATTCTAATACGACTCACTATAGGCCCG-CCTGGAGGCCGC-3' and the reverse primer 5'-GAC-CCGCGGCTGACAGAGC-3'. Both RNA fragments start with two guanosine residues on their 5' end to aid in T7 transcription efficiency. The PCR products were resolved on a 0.8% agarose gel and purified using a Wizard PCR Preps DNA Purification system (Promega). In vitro transcription was carried out at 37 °C for 18 h using the purified PCR products or linearized phTR+HH, 1 unit/ $\mu\text{L}$  T7 RNA polymerase (Promega), 1 × transcription optimized buffer (Promega), 10 mM DTT, 1 unit/ $\mu\text{L}$  RNasin (Fisher Scien-

tific), 5 mM  $\text{MgCl}_2$ , 1 mM ATP, 1 mM GTP, 1 mM UTP, 20  $\mu\text{M}$  CTP, and 0.75  $\mu\text{M}$  [ $\alpha$ - $^{32}\text{P}$ ]-CTP (800 Ci/mmol, 10  $\mu\text{Ci}/\mu\text{L}$ ; Perkin-Elmer). After transcription, the magnesium–inorganic diphosphate complexes were removed by centrifugation for 2 min at 22000g. The addition of  $\text{MgCl}_2$  to the hTR+HH transcription reaction was not required in this protocol as gel analysis revealed that the hammerhead had cleaved during the 18 h incubation at 37 °C. The reaction was then treated with 7 units of RQ1-DNase (Promega) for 20 min at 37 °C followed by extraction with phenol/chloroform/isoamyl alcohol. The RNA was precipitated with ethanol in the presence of 2 M  $\text{NH}_4\text{OAc}$  and resuspended in a suitable volume of TE. A second ethanol precipitation was performed to decrease the amount of unincorporated NTPs. The samples were then passed through Microspin G-25 columns (Amersham) to ensure the removal of all unincorporated [ $\alpha$ - $^{32}\text{P}$ ]-CTP.

**Immunoprecipitation/RNA Pull-Down.** A 75  $\mu\text{L}$  reaction contained 50  $\mu\text{L}$  (~250 fmol) of  $^{35}\text{S}$ -labeled hTERT from a reticulocyte lysate reaction, and 400–900 fmol of  $^{32}\text{P}$ -labeled pseudoknot or CR4–CR5 RNA fragment or full-length hTR (1.3–1.9 × 10<sup>6</sup> cpm per reaction). Inhibition studies also included varying amounts of oligonucleotide inhibitor(s). Reactions were incubated at 30 °C for 90 min to allow binding between the RNA and the protein. Each reaction was immunoprecipitated using 25  $\mu\text{L}$  of anti-T7 antibody agarose beads (Novagen). Before use, the anti-T7 beads were washed four times with 375  $\mu\text{L}$  of wash buffer 1 (20 mM Tris-acetate, pH 7.5, 10% glycerol, 1 mM EDTA, 5 mM  $\text{MgCl}_2$ , 100 mM potassium glutamate, 0.1% IGEPAL, and 1 mM DTT) and blocked twice with 250  $\mu\text{L}$  of blocking buffer (20 mM Tris-acetate, pH 7.5, 10% glycerol, 1 mM EDTA, 5 mM  $\text{MgCl}_2$ , 100 mM potassium glutamate, 0.1% IGEPAL, 1 mM DTT, 0.5 mg/mL lysozyme, 0.5 mg/mL BSA, 0.05 mg/mL glycogen, and 0.1 mg/mL yeast RNA) for 15 min at 4 °C. Between each washing and blocking step, the beads were precipitated by centrifugation at 1500g for 2 min and the supernatant was removed. A total of 75  $\mu\text{L}$  of blocking buffer was then mixed with the 75  $\mu\text{L}$  RNA/protein sample and centrifuged at 17000g for 10 min at 4 °C to remove any precipitates. This supernatant was then added to the blocked beads, and the samples were mixed on a rotary platform for 2 h at 4 °C. Following mixing, the beads were washed three times with 325  $\mu\text{L}$  of wash buffer 2 (20 mM Tris-acetate, pH 7.5, 10% glycerol, 1 mM EDTA, 5 mM  $\text{MgCl}_2$ , 300 mM potassium glutamate, 0.1% IGEPAL, and 1 mM DTT) and twice with 325  $\mu\text{L}$  of TMG (10 mM Tris-acetate, pH 7.5, 1 mM  $\text{MgCl}_2$ , and 10% glycerol). The beads were precipitated by centrifugation at 1500g for 2 min between each wash and the supernatant was removed. The beads were then resuspended in 1 × SDS gel loading buffer containing 10 mM DTT. Samples were heated for 5 min at 95 °C and the supernatant was loaded onto a 4–12% Bis-Tris SDS gel (Invitrogen). The gel was run at 130 V for 1 h, dried, and exposed to a phosphorimager screen overnight. RNA band intensities were quantified, normalized to the  $^{35}\text{S}$ -hTERT protein bands, and compared to the positive control.

**Inhibition Studies.** Direct telomerase or assemblage assays were conducted as described above with varying concentrations of inhibitors. IC<sub>50</sub> values were calculated using the Regression Wizard program of SigmaPlot (version 7.0). Six data points were used with oligonucleotide concentrations



Table 1: Summary of Inhibition Data with hTR-Targeted Oligonucleotides<sup>a</sup>

name	sequence	hTR region targeted	nucleotides <sup>b</sup> targeted	% activity <sup>c</sup>
hTRas001	5'-ATGGCAAGTCCGAATCGATCGT-3'	none	N/A	804
hTRas002	5'-TAGGGTTAGACAA-3'	template (CR1)	42–54	97
hTRas003	5'-AAAGTCAGCGAGAAAAACAGCG-3'	pseudoknot domain (CR2/CR3)	94–115	97
hTRas004	5'-AACGGGCCAGCAGCTGACATTT-3'	P3/P1 pairing region	174–195	37
hTRas005	5'-TGGGTGCCTCCGGAGAAGCCCC-3'	L6 loop	268–289	100
hTRas006	5'-CGGCTGACAGAGCCCAACTCTT-3'	CR4–CR5 domain	301–322	54
hTRas007	5'-GCCTGAAAGGCCTGAACCTCGC-3'	hypervariable paired region	343–364	115
hTRas008	5'-ACAGCTCAGGGAATCGCGCCGC-3'	CR7 domain	397–418	74
hTRas009	5'-AACGGGCCAGCAGCUGACAUUU-3' <sup>d</sup>	P3/P1 pairing region	174–195	12
hTRas010	5'- <u>CGGC</u> UGACAGAGCCCAACU <u>UUU</u> -3' <sup>d</sup>	CR4–CR5 domain	301–322	18

<sup>a</sup> DNA oligonucleotides were added to hTERT and hTR prior to assemblage. Telomerase activity was determined as described in Materials and Methods. <sup>b</sup> Nucleotides within hTR that were targeted by the oligonucleotides. <sup>c</sup> “% Activity” indicates the amount of residual telomerase activity at a 1  $\mu$ M concentration compared to the primer-only control. <sup>d</sup> hTRas009 and hTRas010 are 2'-O-methyl oligonucleotides, and underlined nucleotides indicate phosphorothioate linkages.

ranging from 0 to 10  $\mu$ M. The following four-parameter logistic curve equation was used:

$$y = D + [(A - D)/(1 + (x/C)^B)]$$

where  $x$  is the concentration of inhibitor,  $y$  is the % activity relative to the primer-only control,  $A$  is the maximal activity,  $B$  is the slope factor,  $C$  is the  $IC_{50}$  (i.e., the concentration required for 50% inhibition), and  $D$  is the minimal activity. Inhibition data were plotted as % activity vs log oligonucleotide concentration and fit using the same equation.

**Nondenaturing Polyacrylamide Gel Electrophoresis of <sup>32</sup>P-hTR.** Nondenaturing PAGE was performed using a modification of the protocol described by Ly et al. (35). Briefly, each 10  $\mu$ L reaction contained 0.6  $\mu$ g of unlabeled hTR and about 11000 cpm of tracer <sup>32</sup>P-hTR. The samples were heated at 95 °C for 5 min, immediately placed on ice, and adjusted to 50 mM NaCl, 25 mM Tris-Cl, pH 7.0, 10 mM MgCl<sub>2</sub>. hTRas009 or hTR010 was then added to a final concentration of 10  $\mu$ M. Samples were then either kept on ice or incubated at 37 °C for 2 h to allow for dimerization. Samples were analyzed on a 4% nondenaturing gel in 90 mM Tris-borate, 0.1 mM MgCl<sub>2</sub>. The gel was run at 100 V for 6 h in a cold room (4 °C). After drying the gel and exposing it to a phosphorimager screen overnight, the extent of dimerization was quantified.

## RESULTS

**Identification of Susceptible Regions of hTR.** To define regions of hTR that can be targeted for the disruption of telomerase assemblage, we tested a series of oligonucleotides that were complementary to various regions of hTR for their ability to inhibit reconstituted telomerase activity in vitro (Table 1). Previously, the use of PNAs that were complementary to nontemplating regions of telomerase were shown to inhibit telomerase when added prior to assemblage (21). Because the PNA–RNA duplex is very stable, we thought that the PNAs could change the structure of the RNA subunit to inhibit telomerase as opposed to blocking hTR/hTERT interactions, which we were interested in. For example, a PNA that targeted nucleotides 1–12 was a strong inhibitor of telomerase prior to assemblage (21), even though these nucleotides are not required for telomerase activity (38). This suggests that while the folded structure of hTR was perturbed, specific hTR/hTERT interactions were not inhibited.

We chose to examine DNA oligonucleotides to diminish this effect in an attempt to define regions of hTR/hTERT interactions that can be blocked. Eight DNA oligonucleotides (hTRas001–hTRas008) were screened for their ability to affect telomerase using an assemblage assay. All oligonucleotide inhibitors were maintained at a concentration of 1  $\mu$ M throughout the experiment. A positive control with no oligonucleotide inhibitor was used to determine 100% activity and hTERT-only and hTR-only negative controls were used as controls for background activity (data not shown). We found that only oligonucleotides hTRas004 and hTRas006, which target the P3/P1 pairing region and CR4–CR5 domain, respectively, significantly decreased telomerase activity, defined as <55% residual activity when compared to the positive control. Interestingly, hTRas008, which targets the CR7 domain, was slightly refractory toward telomerase activity (~70% residual activity). We also noted that the addition of a random DNA molecule, hTRas001, resulted in increased telomerase activity (~800%). By contrast, a non-specific PNA inhibited telomerase when added preassemblage with an  $IC_{50}$  = 30  $\mu$ M (21).

**Concentration Dependence of hTRas009 and hTRas010 Inhibition.** To improve hybridization of the inhibitory oligonucleotides to hTR, 2'-O-methyl modifications were made at each nucleotide (39), and to afford increased nuclease resistance, phosphorothioate linkages were incorporated at the ends of each oligonucleotide (40) (Table 1). The modified oligonucleotides were tested for their ability to inhibit telomerase activity in an assemblage assay at a range of concentrations (Figure 2A,B). At high concentration (10  $\mu$ M) of hTRas009 or hTRas010 we observed a new product band in the analysis (lane 6, Figure 2A,B). We therefore carried out an assay with 10  $\mu$ M of oligonucleotide in the absence of a telomeric primer (lane 7, Figure 2A,B). These no-primer controls resulted in the production of the same products (compare lanes 6 and 7, Figure 2A,B), and these artifacts were also produced in reactions catalyzed by reticulocyte lysate expressing an empty vector demonstrating that they are telomerase independent (data not shown). Therefore, the bands in lanes 6 and 7 not attributable to telomerase-catalyzed primer extension were excluded from the  $IC_{50}$  calculations. Both hTRas009 ( $IC_{50}$  = 72.5  $\pm$  15.3 nM) and hTRas010 (163  $\pm$  29.9 nM) were nanomolar inhibitors of telomerase (Figure 2C,D). By comparison, oligonucleotide

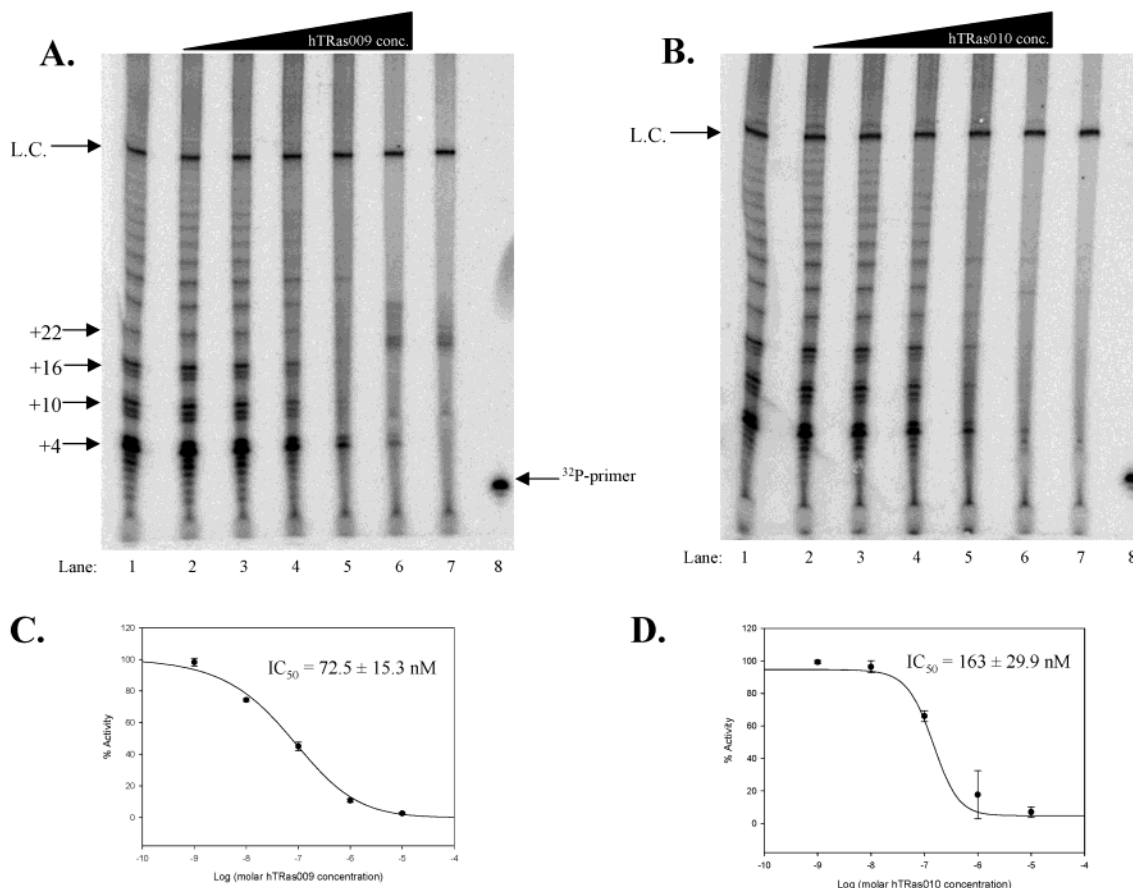


FIGURE 2: Concentration dependence of telomerase inhibition by hTRas009 and hTRas010 when added before assemblage. hTRas009 (A) or hTRas010 (B) were added to an assemblage assay at concentrations of 1 nM, 10 nM, 100 nM, 1  $\mu$ M, and 10  $\mu$ M (lanes 2–6, respectively). Lane 1 is a primer-only control. Lane 7 is a no-primer control. Lane 8 is a <sup>32</sup>P-labeled primer to mark the beginning of primer extension. The <sup>32</sup>P-labeled loading control (L.C.) and the human telomere primer-extension products (+4, +10, +16, +22, etc. nucleotides added) are indicated. IC<sub>50</sub> values were calculated and inhibition curves were plotted for hTRas009 (C) and hTRas010 (D) as described in Materials and Methods. IC<sub>50</sub> curves are based on results from duplicate experiments. Error bars in C and D indicate standard deviation.

inhibitors that target the template portion inhibit telomerase in the low nM range (41), although the concentration of hTR in these assays is much lower than in our assays, making a direct comparison impossible. Importantly, telomerase activity was almost completely eradicated (~5% residual activity) by either oligonucleotide at high concentration (10  $\mu$ M).

**Direct Telomerase Assay in the Presence of hTRas009 and hTRas010.** Telomerase was preassembled *in vitro* and assayed in the presence of either hTRas009 or hTRas010. The direct telomerase assays were conducted in the presence of the two highest oligonucleotide concentrations tested in the assemblage assay (Figure 3). Under these conditions, neither oligonucleotide significantly inhibited telomerase activity when compared to their inhibition in the assemblage assay (59 and 88% residual activity for hTRas009 and hTRas010, respectively, in the direct telomerase assay as compared to ~5% residual activity for either oligonucleotide in the assemblage assay).

**The Effect of hTRas009 and hTRas010 on the Association of hTR with hTERT.** Since hTRas009 and hTRas010 only inhibit telomerase when added prior to assemblage, we hypothesized that they interfere with proper assemblage but do not directly inhibit enzymatic activity. We therefore studied the ability of these antisense molecules to affect binding of hTR to hTERT using a co-immunoprecipitation assay. Because the pseudoknot and CR4–CR5 domains have

previously been shown to interact independently with hTERT (23, 30, 31, 34), we tested each oligonucleotide for their ability to block binding of their respective targeted domains to hTERT (Figure 4). T7-tagged hTERT was translated in the presence of [<sup>35</sup>S]-methionine, which allowed normalization of the co-immunoprecipitation data, and was incubated with <sup>32</sup>P-labeled RNA fragments to allow for RNA/hTERT binding. The resulting complexes were then immunoprecipitated. Controls with no oligonucleotide were performed along with two different concentrations of oligonucleotide (200 nM and 1  $\mu$ M). We found that, in the absence of inhibitory oligonucleotides, the pseudoknot domain (nucleotides 46–209) and the CR4–CR5 domain (nucleotides 243–328) of hTR both independently interact with hTERT, consistent with previous reports (23, 30, 31, 34) (lanes 1 and 4, Figure 4). When the pseudoknot RNA fragment was incubated with hTERT in the presence of hTRas009, co-immunoprecipitation of the RNA with hTERT was inhibited by ~50% (lanes 2 and 3, which are normalized to the <sup>35</sup>S-hTERT signal, Figure 4). Conversely, hTRas010 was able to inhibit binding of the CR4–CR5 RNA fragment by 92% of the maximum binding (lanes 5 and 6, Figure 4).

We tested the effect of hTRas009 and hTRas010 on the association between hTERT and full-length hTR (lanes 7–10, Figure 4). <sup>32</sup>P-labeled hTR (451 nt) was incubated with <sup>35</sup>S-labeled hTERT either alone, with 1  $\mu$ M hTRas009,

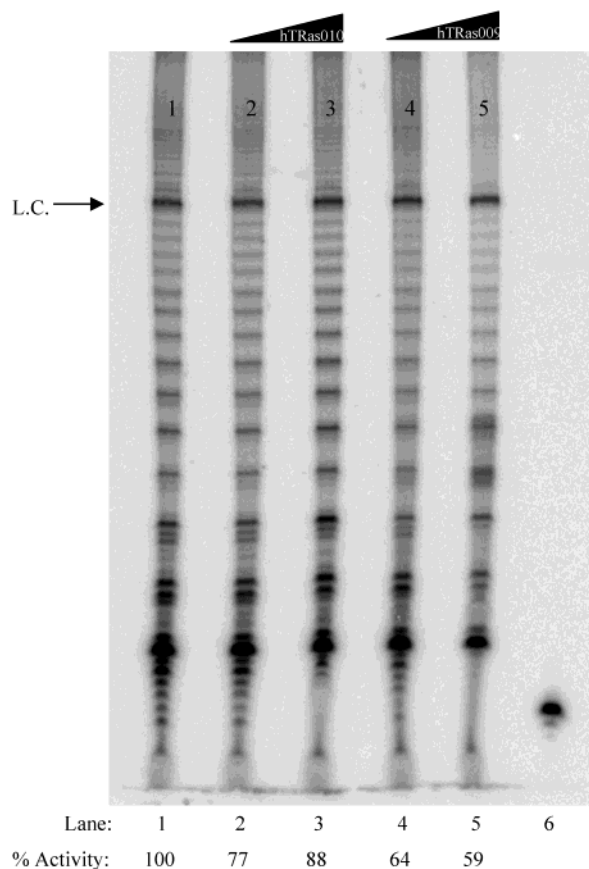


FIGURE 3: Concentration dependence of telomerase inhibition by hTRas009 and hTRas010 when added after assemblage. hTRas010 (lanes 2 and 3) or hTRas009 (lanes 4 and 5) were added to the direct telomerase assay at concentrations of 1  $\mu$ M (lanes 2 and 4) and 10  $\mu$ M (lanes 3 and 5). Lane 1 is a primer-only control. Lane 6 is a  $^{32}$ P-labeled primer to mark the beginning of primer extension. The  $^{32}$ P-labeled loading control (L.C.) is indicated. “% Activity” values indicate the amount of residual telomerase activity as compared to the primer-only control.

with 1  $\mu$ M hTRas010, or with both 1  $\mu$ M hTRas009 and 1  $\mu$ M hTRas010. Compared to the control with no oligonucleotide, hTRas009 and hTRas010 had little effect on the association of hTR and hTERT (compare lanes 8 and 9 to lane 7, Figure 4). However, when both hTRas009 and hTRas010 were present, hTR binding was decreased by ~50% compared to the control with no oligonucleotide (compare lane 10 to lane 7, Figure 4).

To demonstrate the specificity of the oligonucleotides for their respective  $^{32}$ P-labeled RNA fragments, hTRas009 was incubated with  $^{35}$ S-labeled hTERT and the CR4–CR5 RNA fragment, and hTRas010 was incubated with  $^{35}$ S-labeled hTERT and the pseudoknot RNA fragment. We found that neither oligonucleotide was able to block the binding between the RNA and protein compared to the controls with no oligonucleotide (data not shown). Instead, we saw an increase in the association of the RNA fragments with hTERT when the nontargeting oligonucleotide was present. Nonspecific binding was analyzed using an empty vector control. In these samples, less than 5% of the RNAs bound to beads compared to samples containing hTERT (data not shown).

*The Effect of hTRas009 and hTRas010 on hTR Homodimerization.* Recently, hTR was shown to dimerize through an intermolecular interaction between stems of the hTR pseudoknot (35). To determine if hTRas009 or hTRas010

affect hTR homodimerization,  $^{32}$ P-labeled hTR was incubated either in the presence or absence of hTRas009 or hTRas010 at a final concentration of 10  $\mu$ M (Figure 5). As expected, we found that the addition of hTRas010 (lane 4) had no effect on hTR homodimerization as compared to the control (lane 2); however, the addition of hTRas009 (lane 6) decreased dimerization by about 50% as compared to the control. A similar trend in dimerization values is seen for the nonincubated controls (lanes 1, 3, and 5).

## DISCUSSION

The involvement of telomerase in a wide range of cancers has made it an attractive target in anticancer research. Although a complete description of human telomerase and all of its subunits awaits further elucidation, the minimally active complex, a dimer of hTR and hTERT, provides several conceivable approaches for inhibition. In particular, the identification and proposed secondary structure of hTR (22) has opened a number of doors for specific antisense inhibition. Oligonucleotides that are complementary to portions of hTR that target the telomerase holoenzyme have been extensively studied (20), and oligonucleotides that target nontemplating portions have received some attention (21, 42). Here, we investigated the ability to inhibit telomerase activity by abrogating assemblage of the holoenzyme complex. We identified two 2'-O-methyl RNA oligonucleotides that bind to specific regions of hTR and inhibit telomerase activity with  $IC_{50}$  values in the nanomolar range.

We used eight DNA oligonucleotides that are complementary to separate regions of hTR and discovered that targeting the pseudoknot domain at the P3/P1 intersection and the CR4–CR5 domain at the P6.1 stem–loop resulted in the greatest inhibitory effects. A third oligonucleotide, hTRas008, which targets the CR7 domain, also decreased telomerase activity; however, we chose not to follow-up on this result at this time. Interestingly, hTRas001, an oligonucleotide that is not specific for any region of hTR, increased telomerase activity. This unexpected result suggests that a nucleic acid-binding protein or proteins in the reticulocyte lysate are refractory toward telomerase activity and/or assemblage. Because this oligonucleotide does not target any region of the hTR, it was free to interact with other entities in the reticulocyte lysate. This suggests that the addition of random DNA to telomerase reconstitution assays performed in reticulocyte lysates can be used to increase the yield of active complexes. PNAs that are complementary to a wide variety of hTR regions inhibit telomerase when added prior to assemblage (21). By contrast, DNA oligonucleotides were only inhibitory when targeting three specific regions of hTR. This is presumably because DNA oligonucleotides form less stable duplexes that can be out competed by native structures. For example, hTRas002, which is complementary to the template, did not inhibit telomerase even though corresponding PNAs are excellent inhibitors (21). In the case of the DNA oligonucleotide, hTRas002, the inhibitor was unable to compete with the telomeric primer for the template. We therefore concluded that the DNA oligonucleotides we identified in our screen block interactions between hTR and hTERT as opposed to disrupting more stable native hTR structures, though we cannot rule this out.

Ultimately, we decided to conduct further studies on the oligonucleotides targeting the P3/P1 pairing region (hTRas004)



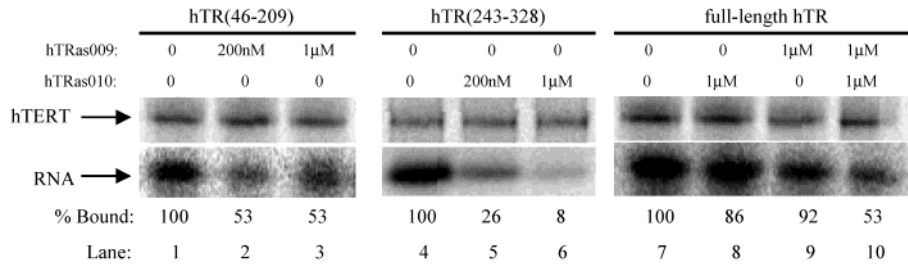


FIGURE 4: Inhibition of hTR/hTERT interactions by hTRas009 and hTRas010. <sup>32</sup>P-labeled pseudoknot RNA fragment (lanes 1–3), <sup>32</sup>P-labeled CR4–CR5 RNA fragment (lanes 4–6), or <sup>32</sup>P-labeled full-length hTR (lanes 7–10) were incubated with <sup>35</sup>S-hTERT either in the presence or absence of oligonucleotide inhibitor(s). The resulting complexes were co-immunoprecipitated and resolved on a denaturing Bis-Tris SDS gel. The [<sup>35</sup>S]-labeled hTERT bands were used as a loading control. hTRas009 was added to an assembly reaction at a concentration of 200 nM (lane 2) or 1 μM (lane 3) to inhibit binding of the pseudoknot RNA fragment. Lane 1 is a control reaction with no oligonucleotide. hTRas010 was added to an assembly reaction at a concentration of 200 nM (lane 5) or 1 μM (lane 6) to inhibit binding of the CR4–CR5 RNA fragment. A control with no oligonucleotide was also performed (lane 4). 1 μM hTRas010 (lane 8), 1 μM hTRas009 (lane 9), or 1 μM each of hTRas009 and hTRas010 (lane 10) was added to an assembly reaction to inhibit binding of full-length RNA. Lane 7 is a control reaction with no oligonucleotide. “% Bound” values indicate the amount of RNA bound to the protein when compared to control reactions with no oligonucleotide. The “% Bound” values in lanes 1–3 are average values from duplicate experiments. Note: The pseudoknot RNA fragment (nucleotides 46–209), CR4–CR5 RNA fragment (nucleotides 243–328), and full-length RNA (451 nucleotides) are different lengths despite the depiction in the figure.

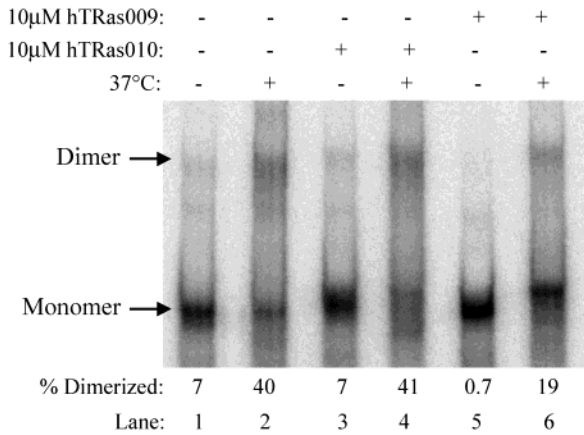


FIGURE 5: hTRas009 inhibits hTR homodimerization. <sup>32</sup>P-labeled full-length hTR was allowed to dimerize either alone (lanes 1–2) or in the presence of 10 μM hTRas010 (lanes 3–4) or 10 μM hTRas009 (lanes 5–6). Samples were either incubated at 37 °C to allow for dimerization (+) or were kept on ice to prevent dimerization (–). “% Dimerized” values indicate the amount of hTR found in the dimer form compared to the total amount of hTR in the sample.

and the CR4–CR5 domain (hTRas006), two regions of hTR that were previously shown to be required for both telomerase activity and the association of hTR with hTERT (23, 29–34). For these experiments, we resynthesized the DNA oligonucleotides with 2'-O-methyl-modified RNA and phosphorothioate linkages on their 5'- and 3'-ends (hTRas009 and hTRas010, Table 1). These alterations increased the inhibitory effects of the oligonucleotides. The increased inhibition can be attributed to the fact that 2'-O-methyl RNA oligonucleotides hybridize to RNA better than DNA oligonucleotides (39). The phosphorothioate modifications were designed for future cell culture experiments in order to decrease oligonucleotide degradation.

In assemblage assays, hTRas009 ( $IC_{50} = 72.5 \pm 15.3$  nM) was found to be a more potent inhibitor of telomerase activity than hTRas010 ( $IC_{50} = 163 \pm 29.9$  nM) (Figure 2). The banding pattern observed is characteristic of human telomerase activity with the first major extension product being four nucleotides longer than the primer and each successive major product having six additional nucleotides. We also noted the presence of unexpected bands in the no-primer

controls revealing that hTRas009 and hTR010, at concentrations of 10 μM, act as substrates for <sup>32</sup>P-dGTP addition by some component of the reticulocyte lysate (lane 7, Figure 2A,B). This observation, however, should not influence the inhibitory effects of the oligonucleotides as the unexpected bands were not seen at lower concentrations. Furthermore, although hTRas009 has a lower  $IC_{50}$  value than hTRas010, both oligonucleotides were able to completely inhibit (~5% residual activity) telomerase activity at the highest concentration tested (10 μM). Notably, the  $IC_{50}$  values for both hTRas009 and hTRas010 are in the same range as the hTR concentration (95 nM) used in the assemblage reactions.

Neither hTRas009 nor hTRas010 significantly inhibited telomerase activity when added after telomerase was allowed to assemble (Figure 3), although hTRas009 inhibited slightly, with 59% residual activity. Perhaps high concentration of hTRas009 can disrupt interactions within the intact telomerase complex. Similar results were found for several PNAs that target nontemplating regions of hTR (21). These results suggest that enzyme activity was inhibited by impeding essential interactions between hTR and hTERT or by disrupting the folding of hTR. Further, our results indicate that the P3/P1 pairing region and the CR4–CR5 domain are not exposed once proper holoenzyme formation is complete. Alternatively, if these domains remain exposed in the holoenzyme, then oligonucleotide interactions after holoenzyme formation do not interfere with activity. Chemical and enzymatic footprinting of hTR revealed that the P6.1 stem-loop, within the CR4–CR5 domain, and the P3/P1 pairing region are protected from cleavage reagents when complexed with hTERT (43). This is consistent with the idea that hTRas009 and hTRas010 cannot hybridize to hTR once the telomerase complex has completely and properly formed.

We tested the hypothesis that hTRas009 and hTRas010 inhibit telomerase by specifically inhibiting interactions between hTERT and the targeted hTR domains. Independent fragments of hTR that are specifically targeted by their respective oligonucleotides were co-immunoprecipitated with hTERT. As expected, we observed that the pseudoknot and CR4–CR5 domains of hTR independently bind hTERT in the absence of oligonucleotide (lanes 1 and 4, Figure 4). hTRas010, which targets hTR at nucleotides 301–322,

hybridizes with the entire P6.1 stem-loop (nucleotides 302–314) and blocks 92% of the binding between hTERT and the CR4–CR5 domain at 1  $\mu$ M (lane 6, Figure 4). This is the expected result if the interaction between the CR4–CR5 domain and hTERT is dependent on interactions with the P6.1 stem-loop, as previously observed by the Greider lab (23). Interestingly, 1  $\mu$ M hTRas009 did not exhibit the same degree of inhibition for the interaction between the pseudoknot fragment and hTERT (lane 3, Figure 4). The fact that hTRas009 was able to decrease the ability of hTERT to bind the pseudoknot fragment by ~50% of the maximum suggests that the region it targets (nucleotides 174–195) is important for protein binding. However, it appears that other regions in the pseudoknot domain (nucleotides 46–209) also contribute to interactions with hTERT.

If hTRas009 does not completely prevent binding of hTERT to the pseudoknot domain, what is its mechanism of inhibition? One intriguing possibility is that hTRas009, which hybridizes to the P3/P1 pairing region, perturbs telomerase activity by interrupting hTR homodimerization. Ly et al. proposed that hTR homodimerization involving contacts in the P3 pairing region results in an essential *trans*-pseudoknot structure (35). They demonstrated that mutants incapable of forming the P3-*trans* interaction were unable to reconstitute telomerase activity but were able to bind to hTERT and suggested that hTR dimerization may provide a foundation for holoenzyme assembly. We tested the ability of hTRas009 to inhibit hTR homodimerization by nondenaturing PAGE. The addition of hTRas009 (lane 6, Figure 5) blocked ~50% of hTR homodimerization as compared to the control (lane 2, Figure 5), whereas the addition of hTRas010 (lane 4, Figure 5) had no effect, as expected. We therefore propose that the mechanism of inhibition of telomerase activity by hTRas009 includes disrupting both RNA–protein interactions and hTR homodimerization. On the basis of this, it is surprising that hTRas003, which targets nucleotides 94–115 in the P3 pairing region of the pseudoknot domain, was not an inhibitor of assemblage (see Table 1). Interestingly, a PNA that targeted nucleotides 93–105 was an inhibitor ( $IC_{50}$  = 0.1  $\mu$ M) of telomerase when added post assemblage, and a PNA that targeted the other portion of the dimerization domain, nucleotides 180–194, was a more potent inhibitor ( $IC_{50}$  = 0.01  $\mu$ M) (21). One explanation is that the PNA targeting nucleotides 180–194 and hTRas009, which targets nucleotides 174–195, form more stable duplex structures compared to the native RNA structure or disrupt important interactions between hTR and hTERT. It is notable that hTR homodimerization was not entirely disrupted. This may be explained by the recent observation that a second RNA/RNA interaction site adjacent to the CR7 domain can contribute to homodimerization (44), which may be related to the observed inhibition by hTRas008. In support of this, Ren et al. showed that an oligonucleotide that targets a similar sequence in hTR inhibited hTR multimerization (44).

To further characterize the effects of hTRas009 and hTRas010 on hTR binding to hTERT, each oligonucleotide alone or both oligonucleotides together were incubated with full-length hTR (451 nt) and hTERT. We found that hTRas009 or hTRas010 alone had little effect on hTR/hTERT binding (lanes 8 and 9, Figure 4). When both oligonucleotides were used in combination, however, 53% of the RNA remained bound as compared to the control,

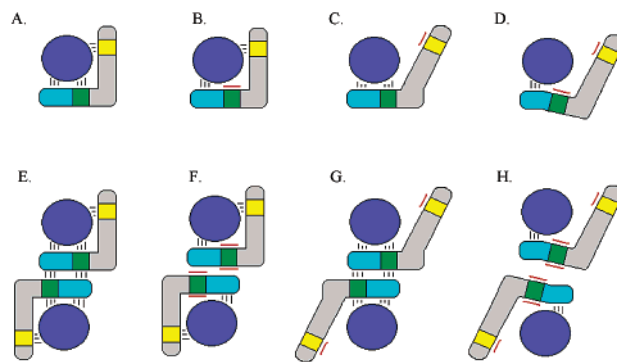


FIGURE 6: hTRas009 and hTR010 prevent proper telomerase assemblage by blocking essential interactions between hTR and hTERT. (A) In the absence of oligonucleotide inhibitor, hTERT (dark blue circle) interacts directly with hTR via the CR4–CR5 domain (yellow), the P3/P1 pairing region (green), and other portions of the pseudoknot domain (light blue). (B) hTRas009, targeting the P3/P1 pairing region, partially blocks hTR/hTERT binding. (C) hTRas010, targeting the CR4–CR5 domain, partially blocks hTR/hTERT binding. (D) hTRas009 and hTRas010 partially block hTR/hTERT binding. (E) Proposed model for telomerase complex dimerization via the P3 pairing regions in the absence of oligonucleotide inhibitor. (F) hTRas009 partially blocks hTR/hTERT binding and blocks dimerization. (G) hTRas010 partially blocks hTR/hTERT binding while dimerization remains intact. (H) hTRas009 and hTRas010 partially block hTR/hTERT binding and block dimerization. Oligonucleotides are depicted by the red lines.

suggesting that other parts of the full-length RNA continued to interact with hTERT (lane 10, Figure 4). Interestingly, the percentage of RNA still bound to hTERT is the same as that in the experiment using hTRas009 alone to inhibit binding of the pseudoknot RNA fragment to hTERT (compare % bound values in lanes 3 and 10, Figure 4). This suggests that the elements of hTR that continue to bind hTERT in the presence of both oligonucleotides reside in the pseudoknot domain (nucleotides 46–209). One explanation for this result is that hTERT interacts with hTR at a minimum of three specific positions and hTRas009 blocks one, hTRas010 blocks another, and the third resides between nucleotides 46–159 as suggested by our work and the work of Bachand et al. (32) (Figure 6).

Our results demonstrate that targeting telomerase holoenzyme assemblage is an effective approach toward inhibiting telomerase activity. Both hTRas009 and hTRas010 had a significant inhibitory effect on telomerase activity in the assemblage assay (Figure 2A,B). However, neither appreciably decreased full-length hTR binding alone (lanes 8 and 9, Figure 4), suggesting that this inhibitory approach not only prevents proper telomerase assembly but also sequesters the telomerase subunits in an inactive state. A model consistent with these data is that hTRas009 and hTR010 prevent proper telomerase assemblage by blocking essential interactions between hTR and hTERT (Figure 6).

Although hTRas009 and hTRas010 were unable to reverse the interaction between preassembled hTR and hTERT to inhibit telomerase activity (Figure 3), their mode of inhibition should be relevant to cancer therapy. In cancer cells, hTR has an extended half-life concomitant with a high transcription rate (45). This suggests that the telomerase complex itself has a high turnover rate. In addition, as cancer cells divide, more telomerase must be generated. Molecules that sequester hTR and induce misassemblage could then have an opportunity to elicit their effects on rapidly reproducing cells.



In fact, it has been demonstrated that PNAs targeting nontemplating regions of hTR can inhibit intracellular telomerase (21). The approach described here to block telomerase assemblage could also provide a chemogenetic method to study telomerase assemblage in cultured cells.

## CONCLUSION

We have identified two oligonucleotides that inhibit telomerase activity in an in vitro reconstitution assay. Our results suggest that their mechanism of inhibition is to induce misassemblage of the telomerase complex by preventing proper binding of essential hTR domains to hTERT. We predict that this approach will provide a method for the in situ generation of a dominant negative telomerase complex.

## ACKNOWLEDGMENT

We thank Dr. Jamie Sperger for the human telomerase RNA plasmid (pHTR+HH), Dr. Lorel Colgin for pCI-neo-hTERT, and Dr. Pamela K. Dominick and Dr. Kenneth Bastow for critical reading of the manuscript.

## REFERENCES

- Rhodes, D., Fairall, L., Simonsson, T., Court, R., and Chapman, L. (2002) Telomere architecture. *EMBO Rep.* 3, 1139–45.
- Cong, Y. S., Wright, W. E., and Shay, J. W. (2002) Human telomerase and its regulation. *Microbiol. Mol. Biol. Rev.* 66, 407–25.
- Meyerson, M., Counter, C. M., Eaton, E. N., Ellisen, L. W., Steiner, P., Caddle, S. D., Ziaugra, L., Beijersbergen, R. L., Davidoff, M. J., Liu, Q., Bacchetti, S., Haber, D. A., and Weinberg, R. A. (1997) hEST2, the putative human telomerase catalytic subunit gene, is up-regulated in tumor cells and during immortalization. *Cell* 90, 785–95.
- Nakamura, T. M., Morin, G. B., Chapman, K. B., Weinrich, S. L., Andrews, W. H., Lingner, J., Harley, C. B., and Cech, T. R. (1997) Telomerase catalytic subunit homologs from fission yeast and human. *Science* 277, 955–9.
- Feng, J., Funk, W. D., Wang, S. S., Weinrich, S. L., Avilion, A. A., Chiu, C. P., Adams, R. R., Chang, E., Allsopp, R. C., Yu, J., et al. (1995) The RNA component of human telomerase. *Science* 269, 1236–41.
- Masutomi, K., and Hahn, W. C. (2003) Telomerase and tumorigenesis. *Cancer Lett.* 194, 163–72.
- White, L. K., Wright, W. E., and Shay, J. W. (2001) Telomerase inhibitors. *Trends Biotechnol.* 19, 114–20.
- Saretzki, G. (2003) Telomerase inhibition as cancer therapy. *Cancer Lett.* 194, 209–19.
- Strahl, C., and Blackburn, E. H. (1996) Effects of reverse transcriptase inhibitors on telomere length and telomerase activity in two immortalized human cell lines. *Mol. Cell. Biol.* 16, 53–65.
- Melana, S. M., Holland, J. F., and Pogo, B. G. (1998) Inhibition of cell growth and telomerase activity of breast cancer cells in vitro by 3'-azido-3'-deoxythymidine. *Clin. Cancer Res.* 4, 693–6.
- Murakami, J., Nagai, N., Shigemasa, K., and Ohama, K. (1999) Inhibition of telomerase activity and cell proliferation by a reverse transcriptase inhibitor in gynaecological cancer cell lines. *Eur. J. Cancer* 35, 1027–34.
- Gomez, D. E., Tejera, A. M., and Olivero, O. A. (1998) Irreversible telomere shortening by 3'-azido-2',3'-dideoxythymidine (AZT) treatment. *Biochem. Biophys. Res. Commun.* 246, 107–10.
- Neidle, S., and Read, M. A. (2000) G-quadruplexes as therapeutic targets. *Biopolymers* 56, 195–208.
- Lyu, S. Y., Choi, S. H., and Park, W. B. (2002) Korean mistletoe lectin-induced apoptosis in hepatocarcinoma cells is associated with inhibition of telomerase via mitochondrial controlled pathway independent of p53. *Arch. Pharm. Res.* 25, 93–101.
- Naasani, I., Seimiya, H., and Tsuruo, T. (1998) Telomerase inhibition, telomere shortening, and senescence of cancer cells by tea catechins. *Biochem. Biophys. Res. Commun.* 249, 391–6.
- Kim, M. Y., Vankayalapati, H., Shin-Ya, K., Wierzbicka, K., and Hurley, L. H. (2002) Telomestatin, a potent telomerase inhibitor that interacts quite specifically with the human telomeric intramolecular G-quadruplex. *J. Am. Chem. Soc.* 124, 2998–9.
- Naasani, I., Seimiya, H., Yamori, T., and Tsuruo, T. (1999) FJ5002: a potent telomerase inhibitor identified by exploiting the disease-oriented screening program with COMPARE analysis. *Cancer Res.* 59, 4004–11.
- Hayakawa, N., Nozawa, K., Ogawa, A., Kato, N., Yoshida, K., Akamatsu, K., Tsuchiya, M., Nagasaka, A., and Yoshida, S. (1999) Isothiazolone derivatives selectively inhibit telomerase from human and rat cancer cells in vitro. *Biochemistry* 38, 11501–7.
- Damm, K., Hemmann, U., Garin-Chesa, P., Haeufel, N., Kauffmann, I., Priepke, H., Niestroj, C., Daiber, C., Enenkel, B., Guilliard, B., Lauritsch, I., Muller, E., Pascolo, E., Sauter, G., Pantic, M., Martens, U. M., Wenz, C., Lingner, J., Kraut, N., Rettig, W. J., and Schnapp, A. (2001) A highly selective telomerase inhibitor limiting human cancer cell proliferation. *EMBO J.* 20, 6958–68.
- Elayadi, A. N., Demieville, A., Wanciewicz, E. V., Monia, B. P., and Corey, D. R. (2001) Inhibition of telomerase by 2'-O-(2-methoxyethyl) RNA oligomers: effect of length, phosphorothioate substitution and time inside cells. *Nucleic Acids Res.* 29, 1683–9.
- Hamilton, S. E., Simmons, C. G., Kathiriyi, I. S., and Corey, D. R. (1999) Cellular delivery of peptide nucleic acids and inhibition of human telomerase. *Chem. Biol.* 6, 343–51.
- Chen, J. L., Blasco, M. A., and Greider, C. W. (2000) Secondary structure of vertebrate telomerase RNA. *Cell* 100, 503–14.
- Chen, J. L., Opperman, K. K., and Greider, C. W. (2002) A critical stem-loop structure in the CR4–CR5 domain of mammalian telomerase RNA. *Nucleic Acids Res.* 30, 592–7.
- Singer, M. S., and Gottschling, D. E. (1994) TLC1: template RNA component of *Saccharomyces cerevisiae* telomerase. *Science* 266, 404–9.
- Blasco, M. A., Funk, W., Villeponteau, B., and Greider, C. W. (1995) Functional characterization and developmental regulation of mouse telomerase RNA. *Science* 269, 1267–70.
- Tsao, D. A., Wu, C. W., and Lin, Y. S. (1998) Molecular cloning of bovine telomerase RNA. *Gene* 221, 51–8.
- Romero, D. P., and Blackburn, E. H. (1991) A conserved secondary structure for telomerase RNA. *Cell* 67, 343–53.
- Lingner, J., Hendrick, L. L., and Cech, T. R. (1994) Telomerase RNAs of different ciliates have a common secondary structure and a permuted template. *Genes Dev.* 8, 1984–98.
- Martin-Rivera, L., and Blasco, M. A. (2001) Identification of functional domains and dominant negative mutations in vertebrate telomerase RNA using an in vivo reconstitution system. *J. Biol. Chem.* 276, 5856–65.
- Mitchell, J. R., and Collins, K. (2000) Human telomerase activation requires two independent interactions between telomerase RNA and telomerase reverse transcriptase. *Mol. Cell.* 6, 361–71.
- Tesmer, V. M., Ford, L. P., Holt, S. E., Frank, B. C., Yi, X., Aisner, D. L., Ouellette, M., Shay, J. W., and Wright, W. E. (1999) Two inactive fragments of the integral RNA cooperate to assemble active telomerase with the human protein catalytic subunit (hTERT) in vitro. *Mol. Cell. Biol.* 19, 6207–16.
- Bachand, F., and Autexier, C. (2001) Functional regions of human telomerase reverse transcriptase and human telomerase RNA required for telomerase activity and RNA-protein interactions. *Mol. Cell. Biol.* 21, 1888–97.
- Beattie, T. L., Zhou, W., Robinson, M. O., and Harrington, L. (2000) Polymerization defects within human telomerase are distinct from telomerase RNA and TEP1 binding. *Mol. Biol. Cell* 11, 3329–40.
- Chen, J. L., and Greider, C. W. (2003) Determinants in mammalian telomerase RNA that mediate enzyme processivity and cross-species incompatibility. *EMBO J.* 22, 304–14.
- Ly, H., Xu, L., Rivera, M. A., Parslow, T. G., and Blackburn, E. H. (2003) A role for a novel "trans-pseudoknot" RNA-RNA interaction in the functional dimerization of human telomerase. *Genes Dev.* 17, 1078–83.
- Colgin, L. M., Wilkinson, C., Englezou, A., Kilian, A., Robinson, M. O., and Reddel, R. R. (2000) The hTERT $\alpha$  splice variant is a dominant negative inhibitor of telomerase activity. *Neoplasia* 2, 426–432.
- Maxam, A. M., and Gilbert, W. (1977) A new method for sequencing DNA. *Proc. Natl. Acad. Sci. U.S.A.* 74, 560–4.
- Ly, H., Blackburn, E. H., and Parslow, T. G. (2003) Comprehensive structure–function analysis of the core domain of human telomerase RNA. *Mol. Cell. Biol.* 23, 6849–56.

39. Monia, B. P., Lesnik, E. A., Gonzalez, C., Lima, W. F., McGee, D., Guinosso, C. J., Kawasaki, A. M., Cook, P. D., and Freier, S. M. (1993) Evaluation of 2'-modified oligonucleotides containing 2'-deoxy gaps as antisense inhibitors of gene expression. *J. Biol. Chem.* 268, 14514–22.
40. Eckstein, F. (2000) Phosphorothioate oligodeoxynucleotides: what is their origin and what is unique about them? *Antisense Nucleic Acid Drug Dev.* 10, 117–21.
41. Corey, D. R. (2002) Telomerase inhibition, oligonucleotides, and clinical trials. *Oncogene* 21, 631–7.
42. Pruzan, R., Pongracz, K., Gietzen, K., Wallweber, G., and Gryaznov, S. (2002) Allosteric inhibitors of telomerase: oligonucleotide N3'→P5' phosphoramidates. *Nucleic Acids Res.* 30, 559–68.
43. Antal, M., Boros, E., Solymosy, F., and Kiss, T. (2002) Analysis of the structure of human telomerase RNA in vivo. *Nucleic Acids Res.* 30, 912–20.
44. Ren, X., Gavory, G., Li, H., Ying, L., Klenerman, D., and Balasubramanian, S. (2003) Identification of a new RNA•RNA interaction site for human telomerase RNA (hTR): structural implications for hTR accumulation and a dyskeratosis congenita point mutation. *Nucleic Acids Res.* 31, 6509–15.
45. Yi, X., Tesmer, V. M., Savre-Train, I., Shay, J. W., and Wright, W. E. (1999) Both transcriptional and posttranscriptional mechanisms regulate human telomerase template RNA levels. *Mol. Cell. Biol.* 19, 3989–97.

BI035583E